Scanning Microscopy

Volume 2 | Number 3 Article 15

6-15-1988

Defect Detection and Thickness Mapping of Passivation Layers on Integrated Circuits Using Energy Dispersive X-Ray Analysis and Image Processing Techniques

Richard G. Sartore
U.S. Army Laboratory Command

Scanning Microscopy, Vol. 2, No. 3, 1988 (Pages 1383-1395)
Scanning Microscopy International, Chicago (AMF O'Hare), IL 60666 USA

DEFECT DETECTION AND THICKNESS MAPPING OF PASSIVATION LAYERS ON INTEGRATED CIRCUITS USING ENERGY DISPERSIVE X-RAY ANALYSIS AND IMAGE PROCESSING TECHNIQUES

Richard G. Sartore*

US Army Laboratory Command (USALABCOM)
Electronics Technology and Devices Laboratory, ATTN: SLCET-RR
Fort Monmouth, N.J. 07703-5302

(Received for publication March 27, 1987, and in revised form June 15, 1988)

Abstract

The relative thickness of passivation layers has been mapped for integrated circuits by utilizing the penetration voltage method, in conjunction with energy dispersive x-ray analysis (EDXA) and a scanning electron microscope (SEM), to detect defects and map film thickness. The thickness mapping technique was evaluated for area coverage and correlated to size of defective areas. The purpose of this study was to determine optimal operational conditions for fast and accurate defect detection on an integrated circuit for failure analysis and non-destructive process evaluation. Image processing was required to enhance the acquired map and to obtain a calibrated image for relative comparison of thickness non-uniformity. Once the defect is detected, linescan and spot measurements can be used to obtain more accurate characterization of the defect areas. Considerable improvement in the detection and characterization of thickness and hole defects in the passivation layers on integrated circuit devices can be obtained with the use of this method.

Key words: Hole defect detection, thickness mapping, thickness non-uniformity, passivation layer, silicon dioxide layer, Scanning Electron Microscope (SEM), Energy Dispersive X-ray Analysis (EDXA), Image processing.

*Address for correspondence:
USALABCOM,
Electronics Technology and Devices Laboratory,
ATTN: SLCET-RR
Fort Monmouth, New Jersey 07703-5302
Phone No.: (201) 544-2261 or AV 995-2261

Introduction

To perform failure analysis and process evaluation on the silicon dioxide insulation layers used in microelectronic devices, the ability to detect defects in these passivation / insulating layers is required. Typically, holes or thickness non-uniformity in the passivation layer can cause device failure or electrical malfunction. These defects can be a micron in size or larger and need to be detected / localized over a relatively large area. Due to the random nature of the defects, the holes in the insulation can occur over metallization run, which in the case of multi-level metal devices would cause a failure. Since multi-level metallization has become an increasingly popular solution for use in VHSIC / VLSI device designs, a high degree of characterization of the insulating layers is required for process evaluation and production monitoring. Besides hole defects, non-uniform thinning of the insulation / passivation layer (over, under or adjacent to high field regions of chip), can be a potential failure site or degrade a device's electrical performance. As a consequence, the ability to characterize the insulation layer both during and after device processing would be extremely beneficial to ultimate device yield and electrical performance.

With this in mind, a program was undertaken to measure the film thickness and to detect / analyze defects (holes and thickness non-uniformity) in insulating layer, by using a scanning electron microscope (SEM) in conjunction with energy dispersive x-ray analysis (EDXA). The objective was to prove the feasibility of the technique and to determine the optimal operating conditions for fast and accurate defect detection and characterization.

Description of Technique

To detect pin holes and thickness non-uniformity in the passivation layer, the penetration voltage method was used. In this method, the acceleration voltage of the SEM is varied until the electrons have enough energy to penetrate the thickness of the film. Once penetration occurs, it is detected by EDXA which identifies the characteristic x-rays from the material under film. If the film on top has a non-uniform thickness, it will show up as a thickness modulated intensity variation of the characteristic x-ray from the sublayer material. By x-ray mapping the characteristic x-ray from the sublayer material

for the area of interest on a microelectronic device, it is possible to visually find a hole defect or non-uniform thickness defect in the insulation over metallization. Typically, image processing is required to enhance the original acquired x-ray map, to highlight and document the defect site. Once the defect area is detected using x-ray mapping, it can be more thoroughly analyzed by using x-ray linescan or spot mode analysis.

Description of Equipment Configuration

The equipment used to implement this technique was: 1) an AMR1700 SEM, with tungsten filament and a continuously variable accelerating voltage, and 2) a Tracor Northern 5500 X-ray analyzer, with Microscan (computer controlled X-Y scan of e-beam) and an image processing package (IPP), for enhancement / analysis of acquired x-ray maps. With this equipment configuration, up to eight elemental x-ray maps can be acquired simultaneously. Typically, only two x-ray maps are required, one for the film material and one for the sublayer material under the film. All acquisitions were taken at a 30 degree take off angle and at sufficient intensity to give either highest intensity x-ray count or 20-30% dead time. The 20-30% dead time criteria was only attainable at the higher accelerating voltages (13 to 15 kV) while the acquisitions at the lower voltages were taken typically at lower count rates (10 to 15% dead time). Acquisition time at each pixel was varied from 0.01 to 0.04 seconds. Most of the x-ray maps were taken at 0.04 seconds to obtain more counts and better resolution of the defects. Since the x-ray map contained 128x128 pixels, acquisition time for one mapped area ran approximately 11 minutes. Various magnifications were used to determine the minimum size of defect detectable. Once the x-ray map was acquired, image enhancement was required. Typically, scaling, background subtraction and image ratio operations were performed on the acquired x-ray map, to enhance x-ray image for better visual analysis on the CRT and for suitable image recording on Polaroid film of the SEM. Without the image processing capability of this system, an attempt to acquire similar images using the standard x-ray mapping capability of the SEM would have required an order of magnitude increase in the acquisition time for just one x-ray map of one element. Further, image processing makes the image ratio capability available. The image ratio technique was found to be particularly useful in enhancing the defect areas. The image ratio divided the aluminum x-ray (Al k-line) map by the simultaneously acquired silicon x-ray (Si k-line) map. The employment of complementary data in the image ratio technique to produce a simulated x-ray map is very effective in highlighting the defect sites while suppressing the background information that is not of interest for this measurement. Smoothing of the x-ray image was also available and proved useful for "noisy" images i.e., images acquired under low count rate conditions or images having a high degree of randomness. The smoothing function averages the pixels with nearest neighbors to produce a more uniform image when the acquisition is done at too low a count rate. The image processing capability proved essential for the implementation of this technique, which would have been impracticable using standard SEM mapping tools.

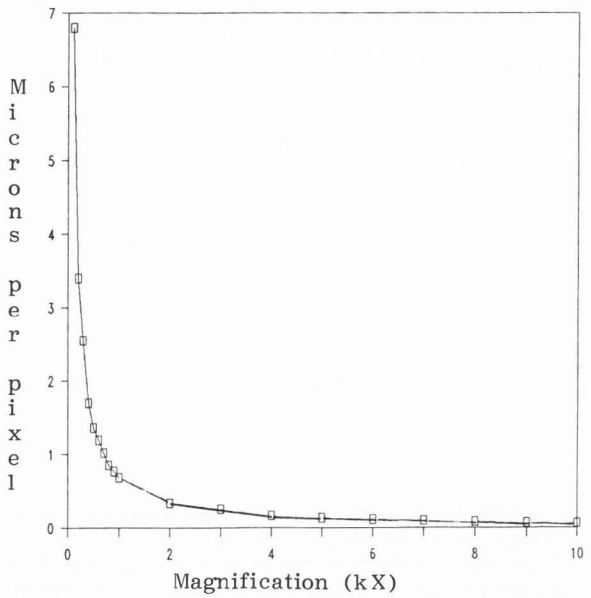

Figure 1. Linear spatial resolution per image pixel (128X128) versus SEM Magnification.

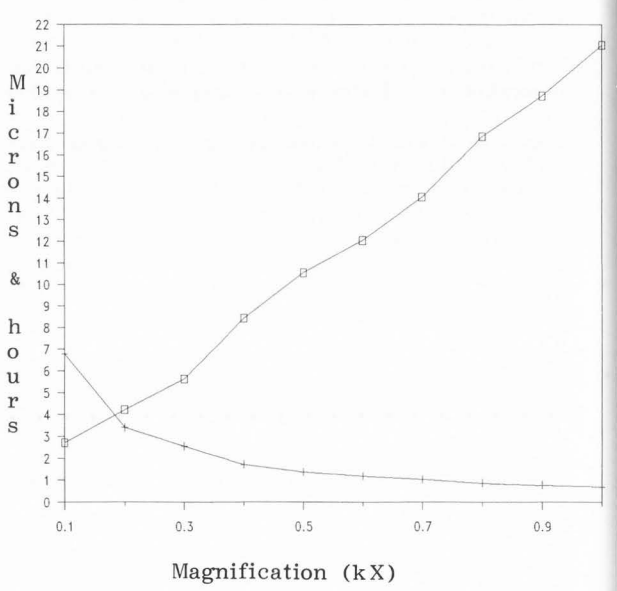

Figure 2. Linear spatial resolution per pixel and time to cover 1 mm square area versus SEM magnification.

Experimental Results

Passivation Defect Detection

Hole Defect Detection. To determine the effective area detectable with the passivation detection technique, a plot was constructed. Calculated data of the linear resolution per pixel was compared against the magnification of the SEM (Fig. 1). From this plot, it is determined that a 1 micron resolution would require a minimum magnification of

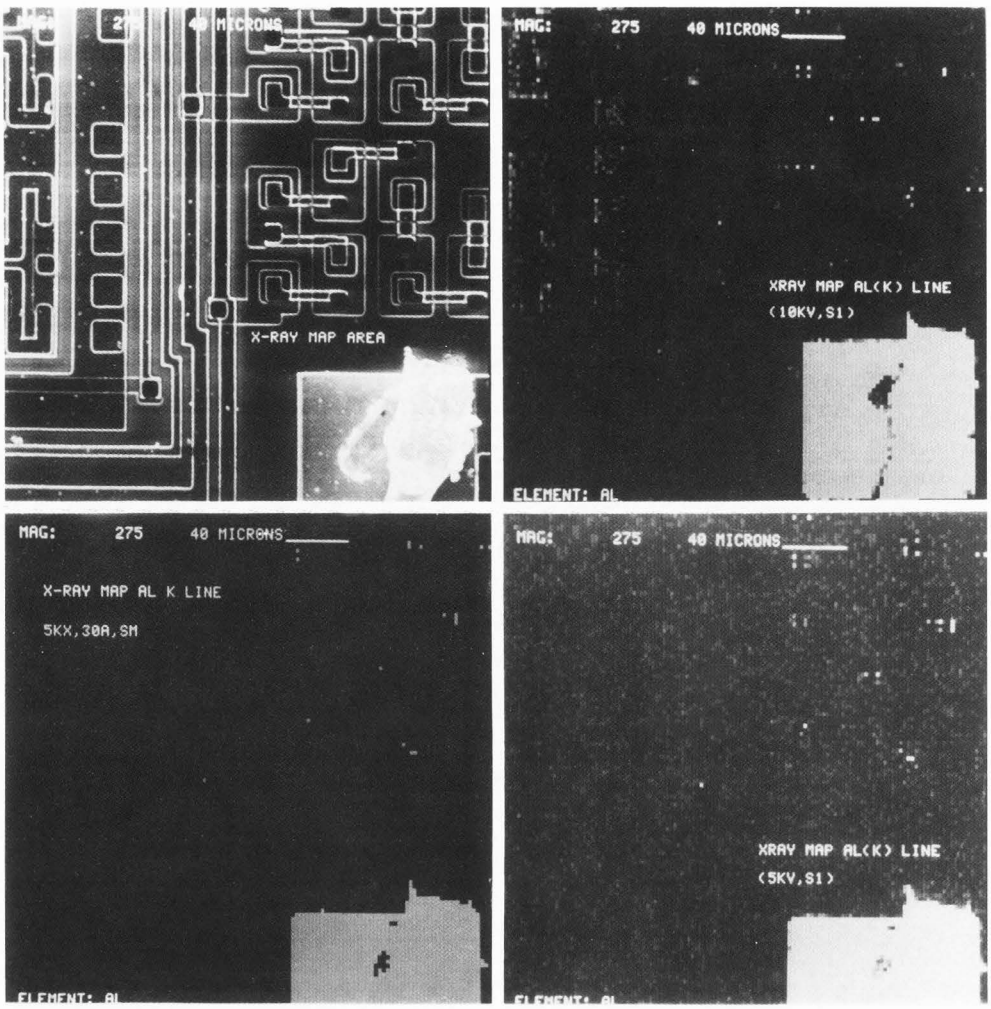

Figure 3. (a, b, c, d, starting from the top left, clockwise):

a) SEM micrograph of x-ray map area,

b) X-ray map of Al (K) line at 10 kV

c) X-ray map of Al (K) line at 5 kV

d) Image processing applied to Fig. 3c)

800x. A two micron resolution would require 400x magnification, see also Postek and Joy, 1987. The corresponding area of chip covered by electron beam scan, using a standard SEM's full scan field, is 125 microns and 250 microns on a side, respectively. Thus, the size of the defect detection requirement is directly proportional to the area covered during electron beam scan. Consequently, the smaller the defect detection requirement, the smaller the area scanned. This proportionality translates into a time requirement of 7 hours for detection of defects with two micron resolution and 14 hours for one micron resolution. These time estimates are based on the assumption that 1 mm square area is to be covered, by successively scanning at the required magnification (400X for two micron resolution and 800X for one micron resolution), with a 0.04 seconds acquisition per pixel. Examples of calculated plots are provided in Fig. 2, where resolution and the time to perform successive scans to cover 1 mm square area is plotted versus the magnification.

When reduction of scan time is desireable, higher count rates can be used with a reduced acquisition time per pixel. Increasing the number of pixels per frame allows a lower magnification to be used for a given defect resolution but will involve essentially the same time for the acquisition of a defect map within a given area due to the acquisition time requirement per pixel. To summarize, high resolution defect detection requires higher magnification with requisite reduction per frame in the scanned area and produces an increased acquisition time for a given area of coverage on the chip. This limitation can be counter-balanced to a degree by increasing the count rate and reducing acquisition time per pixel per picture frame. Thus, by initially specifying defect resolution required and the area to be covered on chip for inspection, it is possible to estimate the time necessary to acquire a set of defect detection maps for the specified area of coverage.

In the acquisition of the thickness or defect detection map, initial consideration must be given to whether a hole defect or thickness non-uniformity is to be measured. Typically, it was found that hole defects were more easily detected at a relatively low voltage (5 kV), due to the fully compensated beam (instrument dependent) providing relatively high beam current / count rates and elimination of background counts from the sublayer material due to low penetration voltage. However, film thickness variation detection and measurement required a higher accelerating voltage as discussed in the next section.

Some typical x-ray maps for Al (K) line at 275X magnification, where varied levels of accelerating voltages were applied, as shown in Fig. 3. The x-ray map taken at 10 kV (Fig. 3b) indicates that there is

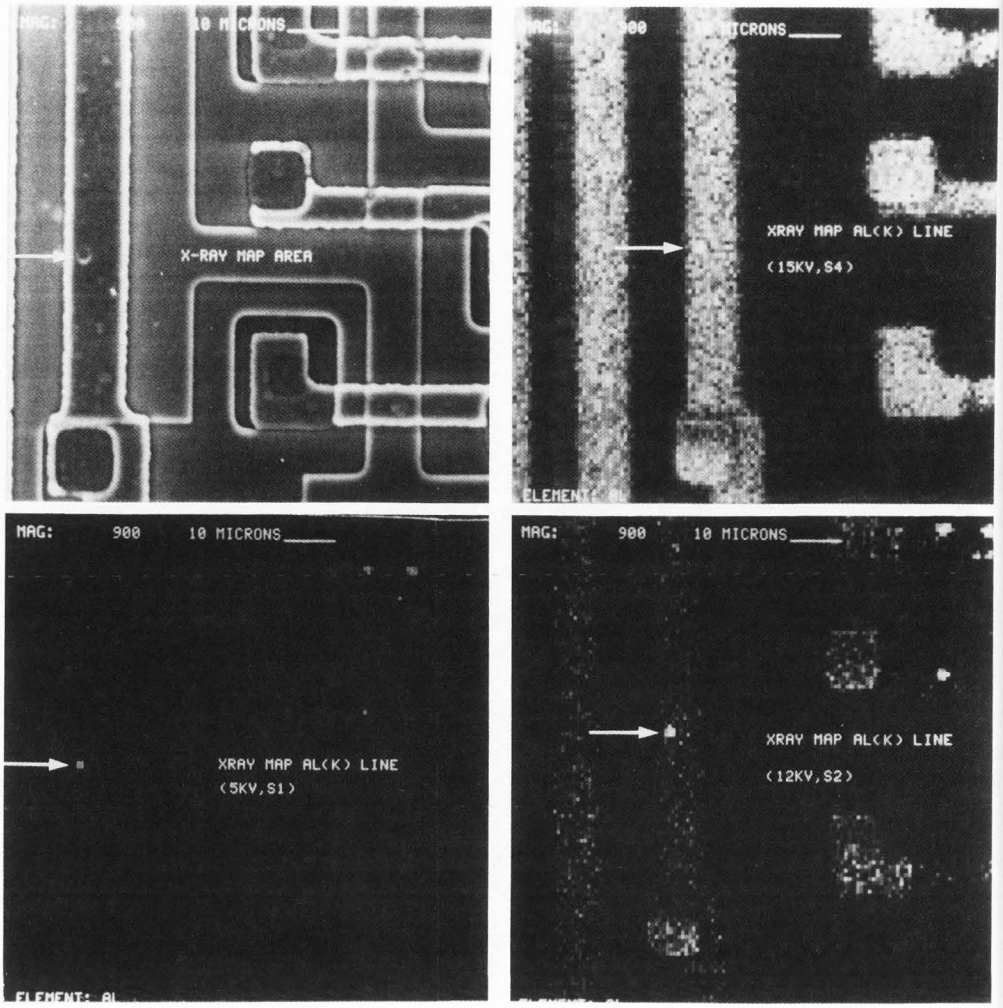

Figure 4. (a, b, c, d, starting from the top left, clockwise)

a) SEM micrograph of x-ray map area,

b) X-ray map of Al (K) line at 15 kV,

c) X-ray map of Al (K) line at 12 kV,

d) X-ray map of Al (K) line at 5 kV.

considerable variation in the passivation thickness over the aluminum metallization lines as shown by the varying x-ray intensity over the surface of the chip. More pertinent for hole defect detection, there are numerous high intensity spots, which tend to indicate hole defect. Due to the large number of possible defects detected with a 10kV map, another map of the Al(K) line was taken at 5 kV to reduce background noise and eliminate consideration of non-uniform thickness and concentrate on hole defects. Fig. 3C is a map (at 5 kV) of the same area as Fig. 3b; extraneous data from the thickness variations have been eliminated at low kV, and therefore locations of hole defects are shown. Fig. 3c was acquired with some scaling and background subtraction to produce an acceptable Polaroid image. With image processing of this x-ray map, the image in Fig. 3d was obtained by taking the ratio of the Al (K) line x-ray map to the simultaneously acquired Si (K) line map, pixel by pixel, and then averaging the nearest neighbor pixels using the smoothing function. This image clearly reduced the background counts and high-lighted the defect areas. This is more clearly seen in Fig. 4, showing the SEM micrograph and x-ray maps of the defect area taken at 900X magnification. The 900X image (Fig. 4a) makes defect sites visible (arrow). From x-ray maps taken at varying accelerating voltages it is readily evident that the higher accelerating voltages, 15kV and 12kV (Figs. 4b, 4c) produce extraneous data with respect to defect detection, which is not evident in the map at 5kV (Fig. 4d). This is due to the fact that the 5kV electrons do not penetrate the passivation film and as a consequence do not produce extraneous sub-layer material counts. However, the higher accelerating voltages do provide information on thickness non-uniformity, as is evident by the increased x-ray intensity at contact areas for the electronic circuit. In summary, to detect hole defects efficiently without including information on thickness non-uniformity, the accelerating voltage should be chosen below the penetration voltage of the film. This is true especially for the case of unprocessed image.

Thus, hole defect detection can be effectively performed at relatively low magnification (400X) to find the holes with 2 micron resolution or better, using low voltage mapping or high voltage mapping with the aid of image processing to suppress extraneous information. This technique is fast and more reliable than the time consuming visual scan of chip surface for insulator or passivation defects. With this method a relatively large area can be analyzed in a shorter period of time and the defect sites effectively high-lighted and detected from the rest of detail / information on the chip. Further, thickness non-uniformity can be detected by observing the

thickness modulated intensity of the x-ray map generated at the higher mapping voltages.

Thickness Non-Uniformity Detection. Detection of thickness non-uniformity in a silicon dioxide film is strongly dependent on the accelerating voltage, which must be selected high enough to have the electrons penetrate the film thickness and to give sufficient x-ray intensity for a statistically significant x-ray map. This is seen in Figs. 4b and 4c, where the accelerating voltages are considerably higher than the film penetration voltage of approximately 8kV. Some quantitative guidelines for selection of suitable accelerating voltages for thickness non-uniformity detection are discussed in the next section. As seen in Figs. 4b and 4c, the x-ray intensity modulation caused by variation in the silicon dioxide film thickness in circuit contact areas, is visually more evident at the higher accelerating voltage, due to higher x-ray intensity attainable for the same acquisition conditions. Image processing techniques will provide additional help in the visual detection of intensity variation of x-ray signal.

In summary, thickness non-uniformity detection is accomplished by visual analysis of x-ray intensity variation in an x-ray map of the sublayer material, with higher accelerating voltages required for sufficient x-ray counts and image processing for image enhancement.

Defect Analysis

Thickness Mapping. To perform analysis of thickness non-uniformities, maps at successively different accelerating voltages can be obtained and rough estimates made as to the voltage required to penetrate the film. The estimated penetration voltage can then be used to estimate the film thickness using the depth-dose range-energy relation (Everhart and Hoff, 1971). With respect to thickness mapping, the beam accelerating voltage must be carefully chosen to penetrate the top film at the specified thickness. Fig. 5 shows a calculated plot of the accelerating voltage of the e-beam for a typical insulator thickness range of silicon dioxide. For the samples used in this report, the penetration voltage was measured to typically vary from 7.5 kV to 8.5 kV, corresponding to thickness variation of 0.6 to 0.8 microns over the surface of consideration. However, in order to obtain sufficient x-ray intensity during the mapping process and thus detect the thickness modulation of the x-ray intensity, it was found that accelerating voltages of 12 kV or higher were needed. This requirement is strictly dependent on the equipment configuration and the need for largest number of counts at each pixel for a given acquisition time. From a qualitative standpoint, the 0.04 seconds per pixel requirement is sufficient for visual detection of hole defects and thickness non-uniformity. From the quantitative analysis standpoint, the limited number of counts at each pixel using the 0.04 second acquisition time, gives a statistically marginal analysis. For higher confidence levels in the quantitative analysis, line scan and point analysis would be required. Calculations of the expected Al (K) x-ray intensity from the sublayer were performed for various thicknesses of silicon dioxide top layers with different accelerating voltages (10-15kV) based on the Everhart and Hoff formulation (Everhart and Hoff, 1971 and Sartore, 1987). Fig. 6 illustrates the plotted data and shows that curves are relatively linear for the higher accelerating voltages (12 kV to 15kV) for the thickness range of interest, namely, 0.5 to 0.95 microns.

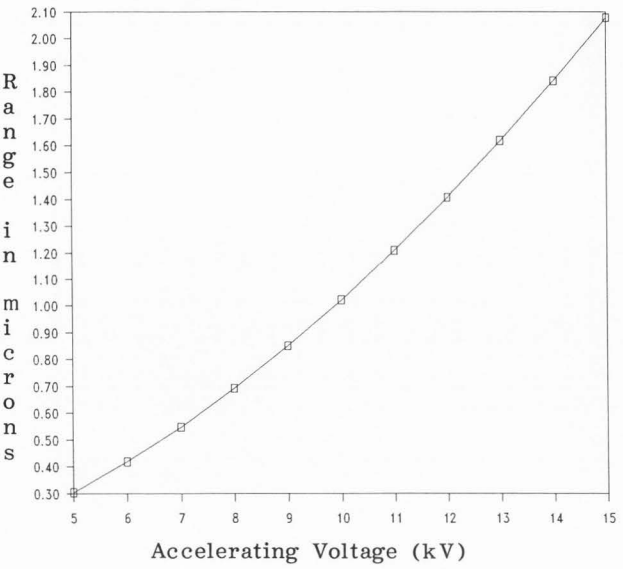

Figure 5. Electron range in SiO_2 (Density = 2.2 g/cm^2) versus SEM accelerating voltage.

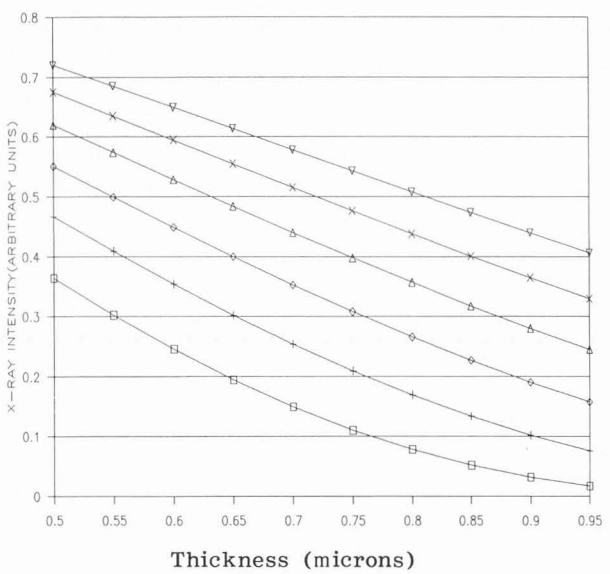

□ 10kV; + 11kV; ◇ 12kV; △ 13kV; x 14kV; ▽ 15kV.

Figure 6. Calculated normalized x-ray intensity from aluminum sublayer versus thickness of SiO_2 top layer for various accelerating voltages in kV (Everhart and Hoff, 1971, and Sartore, 1987).

Fig. 7 presents data, as it was acquired, with pixels scaled to give highest intensity (256 counts) in the hole defect area. Fig. 8 was obtained by taking the ratio of the Al (K) map to the Si (K) map and then smoothing the image. In order to obtain some quantitative information from these acquired and processed images, the relative intensity ratio for a thickness variation equal to 0.2 microns at 0.7

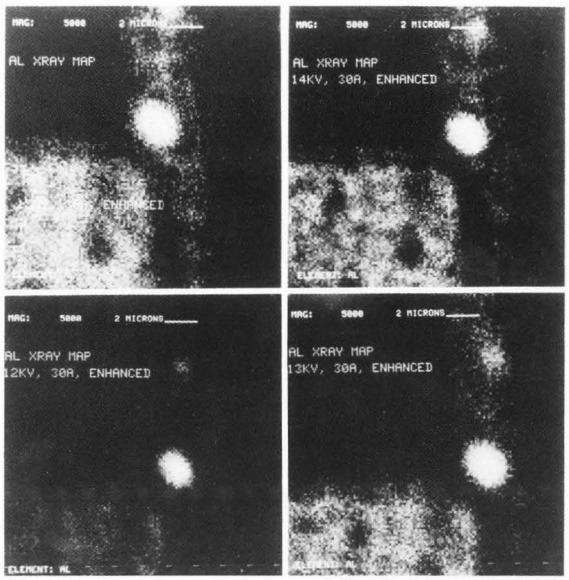

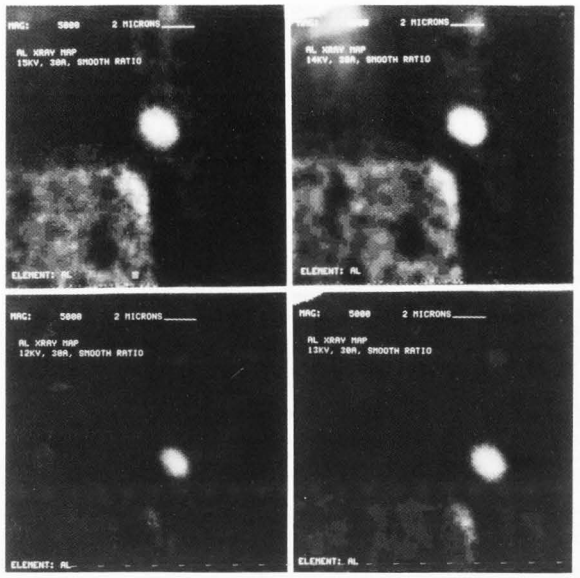

Figures 7 and 8. X-ray map near hole defect, as obtained (Figure 7) and after image processing (Fig. 8). (clockwise, starting from top left) a). 15 kV; b). 14 kV; c). 13 kV; d). 12 kV.

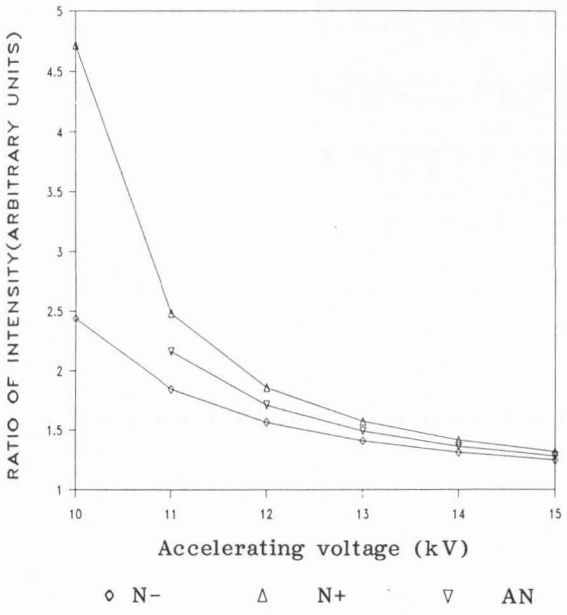

Figure 9. Calculated intensity ratio [N+ = I(0.7) / I(0.9); N- = I(0.5) / I(0.7) and AN = (N+ + N-) / 2) for a thickness variation of 0.2 microns at a nominal film thickness of 0.7 microns versus SEM accelerating voltage (Sartore, 1987).

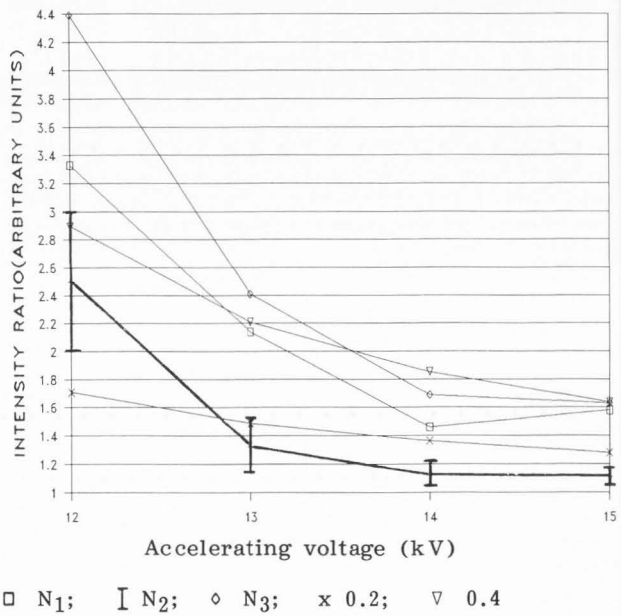

Figure 10. Acquired x-ray intensity ratio data at points N_1, N_2 & N_3 on IC surface compared to normalized calculated intensity ratio for thickness variations of 0.2 and 0.4 microns versus SEM accelerating voltage (error bars on N_2 curve are for +-10 counts).

microns thickness, was calculated for various accelerating voltages and plotted in Fig. 9. N-,N+ and AN were calculated using data from Fig. 6, where AN is the average of the N- and N+ curve. N- corresponds to the 0.5 to 0.7 micron thickness variation (N- equals I_{Al} [at SiO_2 equals 0.5 microns] / I_{Al} [at SiO_2 equals 0.7 microns]); whereas the N+ relates to the variation on the positive side of 0.7, i.e., N+ equals I_{Al} [at SiO_2 equals 0.7 microns] / I_{Al} [at SiO_2 equals 0.9 microns]. As shown by Fig. 9, a thickness variation of plus or minus 0.2 microns, at 0.7 micron thickness, should be detected with an averaged AN curve when using accelerating voltages from 12 to 15 kV. The relatively modest error rate will increase however, once the accelerating voltage is lowered.

Application of this methodology to previous

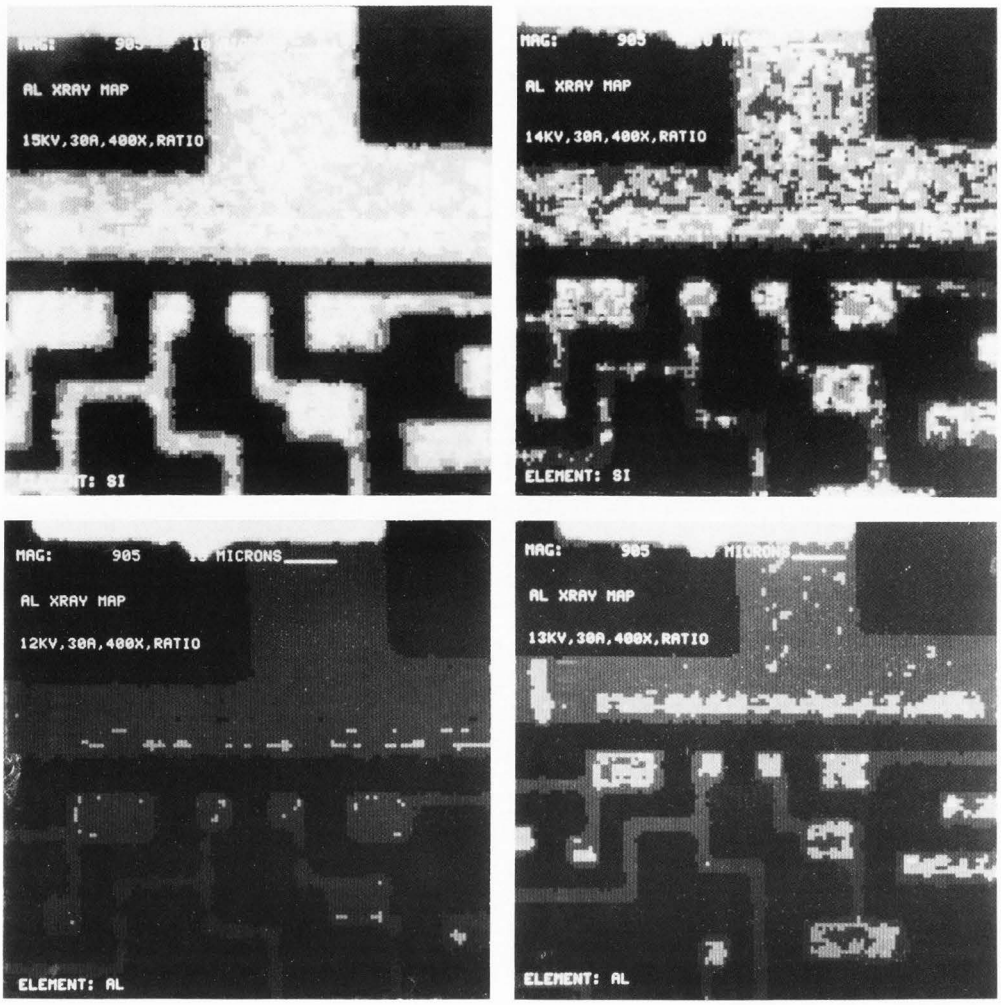

Figure 11. Al x-ray maps near aluminum bond pad. (a, b, c, d starting from top left clockwise):

a). 15 kV;

b). 14 kV;

c). 13 kV;

d). 12 kV.

x-ray maps (Figs. 7 and 8) was employed, on three locations on each of the x-ray maps. The "as acquired" (un-processed) data for several pixels about each location are plotted in Fig. 10, for three data points N_1, N_2, and N_3 in the contact area versus the thicker film over the metal line, N_{ref}, and compared to calculated thickness variations plots of 0.2 and 0.4 microns at nominal thickness of 0.7 microns. The ratio of number of counts at N_1, N_2 and N_3 to the average number of counts at the thicker film over metal line are the values plotted on the vertical axis. This compares to a measured thickness variation of 0.18 microns at N_2, using the penetration voltage method. The discrepancy in the fit to calculated values is attributed to the low number of counts obtained at each pixel in the x-ray mapping process. Due to the poor statistics at each pixel, just a pixel count change of plus or minus 1 will translate into a large variation in the plot obtained from the acquired data. This can be overcome by increasing the acquisition time at each pixel, which in turn carries a penalty of increased mapping time. However, the present method does give a rough estimate of relative thickness variation for qualitative evaluation.

An alternative technique is to acquire an x-ray signal in an area where pure aluminum is present, so that the aluminum can be used as a reference point. This has been done for the example shown in Fig. 11, where the aluminum bond pad is included in the x-ray map. The aluminum bond pad is assigned the maximum normalized x-ray intensity of 1, using image processing techniques, which is represented by 256 counts/pixel. The variable thickness of the silicon dioxide film will produce a modulated intensity with respect to the pure aluminum that can be compared directly with calculated intensities. This is illustrated in Fig. 12, where N_1 is the measured x-ray intensity at point 1, and 1.45 * N_1 is the absorption corrected term for to N_1 (Armstrong, 1978). The +d and -d were used to represent a count variation of ± 10 counts about N_1 corrected for absorption, while 0.8 and 0.75 microns reflect the predicted curves for the indicated thickness of the SiO_2 film. The correlation over voltage range is fairly good and part of the discrepancy can be attributed to poor statistics of the x-ray map and localization of the cursor for successive data measurements. However, the confidence level of the predicted thickness is not as good as the relative thickness measurements previously described. This is true even though the thickness was measured with the penetration voltage method (Sartore, 1987) to be 0.78 microns at point one versus the value of 0.8 microns obtained from Fig. 12, using a calculated absorption correction

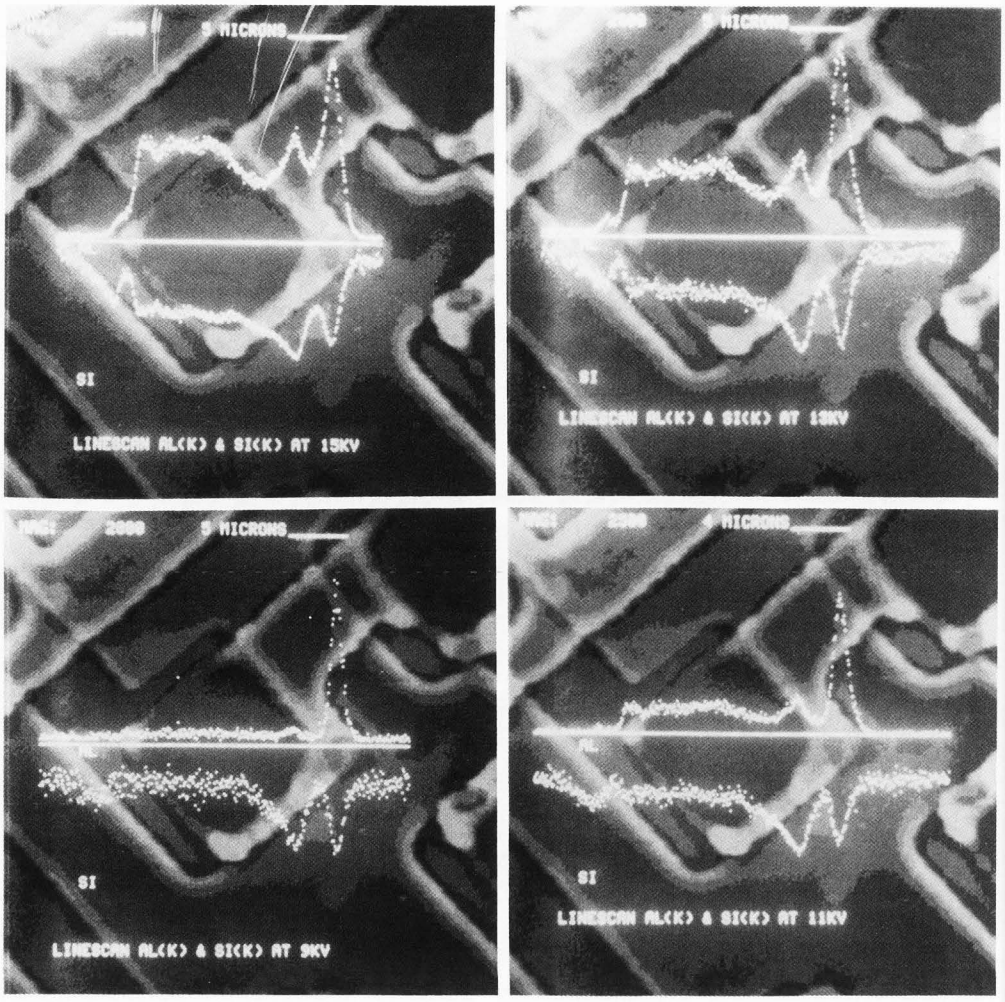

Figure 13. Line-scan of contact area with hole defect on edge (a, b, c, d starting from top left, clockwise):

a). 15 kv.

b). 13 kV.

c). 11 kV.

d). 9 kV.

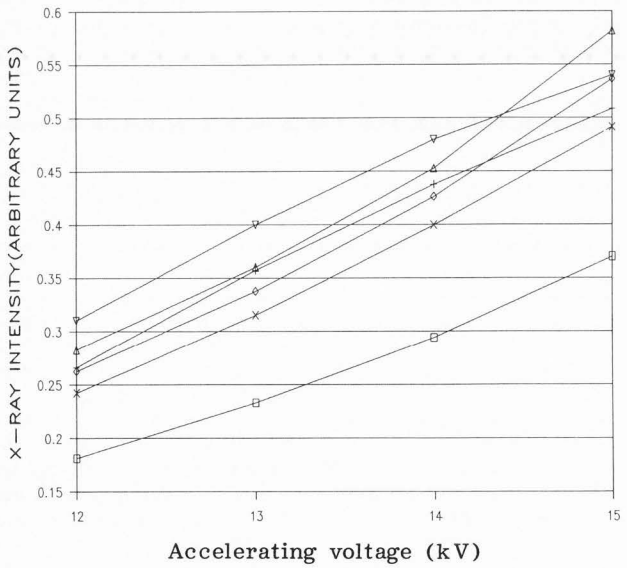

□ N_1; + 0.8 μm; ◊ 1.45*N_1; Δ +d; x -d; ▽ 0.75 μm

Figure 12 (at left). Acquired normalized x-ray intensity data (N_1, lower curve), compared to the calculated intensities for SiO_2 thicknesses of 0.75 and 0.8 microns, and absorption corrected data, with error bands +d and -d (corresponding to counts variation of +10 and -10), versus accelerating voltage.

factor of 1.45. The increased uncertainty is caused by the estimation procedure for correction factor over the multiple accelerating voltage range, in addition to the high accelerating voltages and sparse data previously mentioned.

In summary, the utilization of the x-ray mapping technique to analyze the thickness variation of the silicon dioxide film over aluminum metallization provides relative information concerning the thickness differences in the area of the x-ray map. Quantitative values can be assigned to the thickness variations by comparing the intensity ratios from one area to another on a given x-ray map, to calculated ratios. The accuracy of this method is dependent on the statistics obtained for each pixel and the localization of the e-beam for successive measurements. Further, by including pure aluminum in the x-ray map area, a reference point can be established so that absolute thickness estimates can be made of the silicon dioxide thickness. Again the accuracy of this

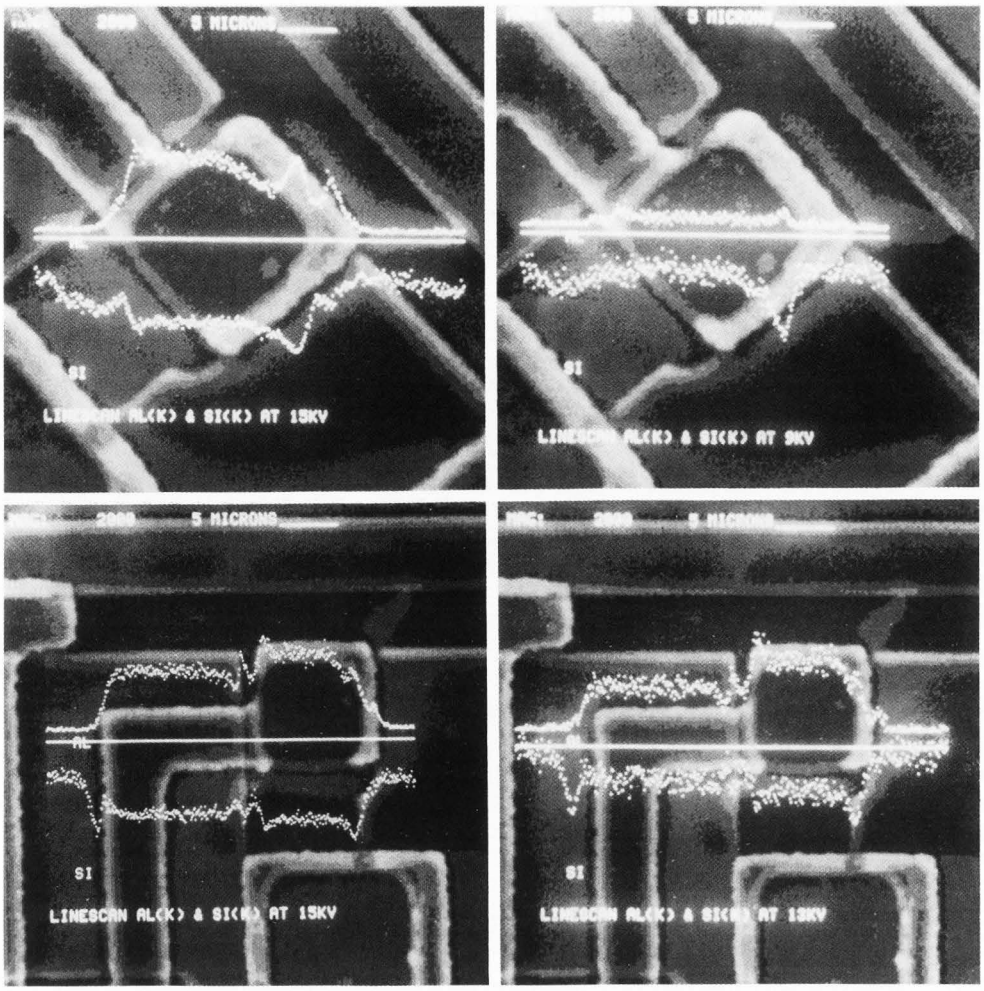

Figure 14. Linescan of normal contact area (a, b) and passivation over metal run (c, d).

(a, b, c, d starting from top left, clockwise).

a). 15 kV.

b). 9 kV.

c). 15 kV.

d). 13 kV.

estimation is dependent upon statistics easily obtainable for each pixel, the localization of the e-beam for successive measurements and the high background counts generated by the relatively high accelerating voltages required for practical implementation of the technique. These methods, of necessity, only give rough estimates of the relative and absolute thickness of the silicon dioxide film over the aluminum metallization. If more accurate estimates of the film thickness are required, a more detailed analysis will have to be performed using linescan or spot analysis.

Linescan Analysis. To obtain better statistics and measurements after the initial detection and rough thickness estimation described in the thickness mapping technique, linescans of the area of interest can be acquired. Acquisition by linescan allows the accumulation of better statistics for a smaller overall number of acquisition points over a reduced area, i.e., a specified line. In the subsequent images, the position of the linescan is indicated by the bright bar superimposed on a digitized image of the area of the integrated circuit that is being analyzed. The digitized image is composed of 256 X 256 pixels and has been processed to reduce contrast at edges of the step features on the integrated circuit, to highlight linscan information. The linescan of the aluminum Al (K) line is displayed above the bright position bar, while the linescan of the silicon Si (K) line is displayed below the position bar. A series of linescans at different accelerating voltages are shown in Fig. 13, for a contact area with a hole defect near the edge. Two elements were acquired simultaneously, aluminum and silicon. The increased detail is evident, with the hole defect giving a high aluminum count and a dip in the silicon curve. Some of the other peaks in the aluminum and valleys in the silicon scan can be attributed to the step coverage of the silicon dioxide, although the correspondence is not one to one, i.e., the aluminum peaks are more pronounced than the valleys in the corresponding silicon line scans.

Some of this discrepancy could be due to geometry, since detector is to the right with a 30 degree take off angle. Additionally, feature sizes might also be significant as discussed for quantitative analysis of small particles (Armstrong, 1978). A detailed investigation of the cause for these discrepancies was not pursued for this work. Comparison of a linescan to a similar contact area without a hole defect is illustrated by Figs. 14a and 14b. Again some of the structure can be correlated as due to step coverage, i.e., thinning of the silicon dioxide at the step. A

more evident example of step coverage is shown in Figs. 14c and 14d, where the correlation between the aluminum and silicon linescan is more nearly one to one at the step appearing in the center of the scan. This better correspondence can be attributed to the more gradual slope of the step as compared to the abrupt steps around the contact area in the previous example.

From a process evaluation or failure analysis standpoint, the ability to qualitatively characterize or compare step coverage is a continuing problem. The linescan technique provides a convenient method for step coverage characterization by comparison. It also provides rough estimates of the relative difference in thickness of the silicon dioxide film at the step compared to the flat area of the chip.

Presence of the hole defect (Fig. 13) enabled an absolute thickness estimate of the silicon dioxide in the contact area by calibrating measurements to the aluminum peak at hole defect to a value of one, pure aluminum (see description, previous section). Estimated results were similar, but greater error was detected (0.7 micron versus a penetration voltage measurement value of 0.64 microns) probably due to feature size effects. But when an aluminum pad area was used for calibration, the results were the same as in the previous section, i.e., linescan analysis of location one in Fig. 11, confirmed the approximately 0.8 micron thickness mapping values obtained in previous section, for location one in Fig. 12.

Further, the thickness variation in Figs. 14c and 14d was estimated to be approximately 0.2 microns versus a measured variation of 0.18 micron using the intensity ratio plots of Fig. 10. Again as described in the previous section, the cause for the inaccuracy can be attributed to: the relatively high accelerating voltages used with this measurement technique versus the penetration voltage method; the subsequent increased background count that would distort the true intensity ratios; and absorption effects that would reduce detected x-ray intensity.

In summary, the linescan analysis provides better statistics and localization in the analysis of the thickness variations of a silicon dioxide film on a microelectronic device. The better statistics acquired in an area of interest will provide a more accurate determination of the intensity ratio of the thickness modulated x-rays from the sublayer material for two different silicon dioxide thicknesses. By comparing this measured intensity ratio to a calculated ratio, the thickness variation between the two locations can be estimated. The relative difference in film thickness can be measured fairly accurately with this method, within plus or minus 0.05 microns. However, this technique was not as accurate for absolute thickness measurement since larger measurement differences were noted between measurements obtained through the penetration voltage method as compared with those from the technique described in this paper. With respect to step coverage analysis, the linescan technique was shown to be particularly effective for detecting thinning of film at steps with gradual slopes. Abrupt steps were not as straight forward from an analysis standpoint and raised some questions with respect to detector geometry and feature size effects. However, use of linescan analysis for step coverage characterization is convenient for comparative analysis of step coverage.

Conclusion

The defect detection capability of the methods described in this paper are particularly applicable to modern microelectronic devices that require multilevel metallization. The hole defect capability is needed to detect holes in insulation over metallization runs. The technique described in this paper can be used at low accelerating voltages to minimize the damage to sensitive electronic elements, such as, MOS technology. In terms of area of chip covered, defect size resolution, and time for analysis, the method described in this paper is a considerable improvement over a standard SEM visual analysis. Image processing capability of the EDXA system was essential for the practical implementation of these techniques. From a productivity standpoint, use of these techniques will allow analysis in a practical time frame with better quality results and higher confidence levels.

Secondly, thickness non-uniformity in the insulation layer over metallization can be detected visually, using the method described in this paper. Further, by measuring the intensity ratio from one location to another and comparing it to calculated values, an estimate of the thickness variation from one location to another can be made. The accuracy was measured to be within +-0.05 microns, provided linescan / point analysis or reasonable statistics (measurable counts) were obtainable at each pixel of the thickness map. The "as acquired" thickness map was image processed to enhance thickness variation by using image ratios and smoothing functions. The image processed thickness map highlighted the relevant thickness variation areas for visual detection and analysis. The importance of detection and analysis of the thickness non-uniformity is due to potential time dependent damage to electrical operation of the microelectronic circuit from higher than anticipated electric field gradients at a thinned insulation site. Repeated electrical stress of a marginal insulator thickness can lead to failure by electrical breakdown and subsequent electrical short. The detection and verification of such failure sites is critical to failure analysis and reliability improvement.

Finally, another repeated problem in the evaluation of microelectronic device quality has been the characterization of step coverage. Visual analysis of step coverage is time consuming and localized to edge of the step. By utilizing the thickness mapping technique in conjunction with linescan analysis, it is possible to obtain profiles of the step coverage in the center or any other position of the line to be evaluated.

It is anticipated that the techniques described in this paper would be suitable for inclusion in MIL-STD-883, Method 2018.2, (1983) where microelectronic circuits are inspected with SEM for quality defects, such as, passivation defects and step coverage.

Acknowledgements

I thank Marilyn B. Riehl for layout and editing of this manuscript.

References

Armstrong J (1978). Methods of quantitative

analysis of individual microparticles with electron beam instruments. Scanning Electron Microsc. 1978;I: 455-467.

Everhart T, Hoff PH (1971). Determination of keV electron energy dissipation versus penetration distance in solid materials. Journal of Applied Physics 42, 5837-5846.

MIL-STD-883C (25 Aug 83). DOD, test methods and procedures for microelectronics, Method 2018.2, scanning electron microscope (SEM) inspection of metallization (4 Nov 1980). Naval Publications and Forms Center, 5801 Tabor Ave., Philadelphia, PA 19120

Postek MT, Joy DC (1987). Submicrometer microelectronics dimensional metrology: scanning electron microscopy. Journal of Research of the National Bureau of Standards, May-June 1987, 92, 205-228.

Sartore R (1987). Measurement of film thickness on integrated circuits using energy dispersive x-ray analysis (EDXA). Scanning Microsc. 1, 41-49.

Discussion with Reviewers

W. J. Hamilton: It has been a common observation in using electron beams for IC examination that energies above 1 to 2 keV can permanently damage many circuits, particularly FETs. Surface oxides can readily be charged to the primary beam accelerating voltage (when the voltage is such that the electron yield is less than one) with resultant damage to the circuit or at least to the measurement process. In the past, x-ray analysis has been precluded not only by the reduction of the accelerating voltage by this screening in unpredictable ways, but also by limitation of the incompatibility of low voltage with the x-ray absorption edge requirements and the low sensitivity of the x-ray methods, particularly EDXA. Since you state that these studies were both for "failure analysis and non-destructive process evaluation", what effect on circuit performance does application of this technique have on various types of devices? For what types of circuits do you recommend the use of this procedure?

H. Oppolzer: Since electron beam voltages of 10 keV to 15 keV are not considered to be low for IC inspection, was damage or degradation of the circuits observed after x-ray mapping for defect detection?

Author: MSI bipolar devices have been examined in this laboratory at 15keV accelerating voltages for extended periods with observation of minimal electrical degradation. LSI and VLSI bipolar devices should be similarly robust under the higher accelerating voltages. However, a testing strategy to minimize exposure and a concomitant charge build-up would be beneficial.

With respect to MOS devices, voltages at 10 to 15 keV would be destructive. Therefore, full thickness characterization for MOS devices, using this technique, must be conducted on a sampling basis. However, in the case of hole defect detection, accelerating voltages below 5keV could be used with minimal effect on threshold voltages (Measurement of deep penetration of low-energy electrons into metal-oxide-semiconductor structure, K. Nakamae, H. Fujioka and K. Ura, J.Appl.Phys., 52(3), p.1306-1308, Mar. 1981). From a practical standpoint, a trade-off, which is dependent on equipment configuration, must be made between lowest possible accelerating voltage and highest possible x-ray intensity from the underlying aluminum metallization, for the case of hole defect detection.

W. J. Hamilton: From the dead-time data and scanning rates stated, it can be estimated that the count rates used in this study are on the order of a few tens to a few hundreds per second. This implies "three sigma" error ranges of 40 to 60 % of the counts. The large variation in the counts is clearly visible in the grey-level fluctuation in Figs. 3c, 4b, 4c, 7a-d. A number of bright pixels which appear in Fig. 3c (5 kV), do not appear in Fig. 3b (10 kV); if these were "holes" in the passivation, as implied, the bright pixels should appear in the higher voltage micrographs whenever they appear in the lower voltage images. Is this lack of correlation from one voltage micrograph to another due to statistical events and not defects?

Author: Although statistical considerations are important, the apparent lack of correlation is primarily due to peculiarities of instrumentation and image processing. Specifically, some of the micrographs at the different voltages could not be taken at exactly the same magnification or x-ray intensity, as the previous micrographs and may include some additional chip structure or brightness. Further, all x-ray images were processed to provide acceptable photographs. This processing is performed manually at present, to provide the highest intensity image at the aluminum bond pad. Some variation was encountered in filming the processed image and accounts for some of the variation noted. Part of the problem at higher accelerating voltages (10 to 15 keV) is the increase in the "background" counts due to the penetration of SiO_2 film with subsequent lowering of "P/B" ratio and compression of the dynamic image range. The increased "background" count presents a visual distortion when the image is enhanced due to the smaller dynamic range and requirement to suppress extraneous data from "background" or thickness non-uniformity during detection of hole defects. This was the case for the examples questioned in the photographs, since original x-ray maps show very good correlation from one voltage to another, when due consideration is given to variations in registration, magnifications and image processing parameters. This is one of the reasons that lower voltages are recommended for hole defect detection, to increase the "P/B" ratio and to reduce extraneous data concerning thickness non-uniformity.

With respect to statistical significance, it is dependent on x-ray intensity, dwell time / pixel, etc. The dwell time was chosen experimentally to give a significant "P/B" ratio for hole defects, typically of 5 to 10. The statistical significance problem becomes meaningful in the measurement of thickness non-uniformity and the prediction of the relative thickness differences.

W. J. Hamilton: The computations of Fig. 2 appear to include only the dwell time of the scanning beam; can these be recomputed to include a figure of merit on the certainty of detection of a "hole" at stated resolution, given the assumed count rate, dwell times, etc?

H. Oppolzer: What level of confidence for defect detection was obtained? How did the number of defects detected on $1mm^2$ chip area compare to values

of other techniques, including destructive ones?
Author: The prime indicator of confidence for hole defect detectability was the "P/B" ratio, which was set experimentally at 5 to 10 at an area near a bonding pad, before acquiring x-ray maps. Assuming that the magnification is chosen properly for the desired spatial resolution i.e. one pixel per defect size and the SEM settings are stable during the acquisition process, there is a high degree of confidence that a defect will be detected. Assuming a detectability limit of a peak (Al) count that is three time the standard deviation of the "background" count, the "P/B" greater than 5 criteria gives a confidence limit of greater than 95% for detectability of the hole defect. Ratioing the simultaneously, complementary acquired data from Al (K) and Si (K) maps will provide further confidence of hole defect detection due to suppression of "background" counts and enhancement of the hole defect.

With respect to other techniques, the typical ones used are visual (optical and SEM) and a destructive chemical technique (MIL-STD-883C, (25 Aug 83),DOD, Test methods and procedures for microelectronics, Method 2021.2, Glassivation layer integrity (15 Aug 1984), Naval Publications and Forms Center, 5801 Tabor Ave., Philadelphia, PA 19120). The visual techniques are time consuming, with specified magnification of 200X for optical inspection and up to 10kX for SEM inspection at the destructive higher accelerating voltages. Due to the multiplicity of features on the optically and SEM inspected devices, automated hole detection would be extremely difficult to implement, as opposed to the technique described in this paper. Further, with proper selection of SEM operating parameters, the technique described in this paper is non-destructive for hole detection, as opposed to the chemical etching method.

W. J. Hamilton: The total time for acquisition (not including image processing) is 7 to 14 hours per mm^2. Would you comment on the utility of the technique as a real-time in-process screening technique? How would this be impacted by even longer times to give greater statistical assurances of defect detection?
Author: The long acquisitions do present difficulties in real time applications. A sampling procedure per lot would be one way of dealing with this problem. Another is to scan only critical areas of interest, such as, metallization crossovers, to reduce the area scanned and, as a consequence, the time for analysis.

V. D. Bui: For submicron pin hole detection under SiO_2, it is very difficult to pin point the site because of the limit of x-ray resolution and penetration of electron beam as well. The two examples below stress the importance of acceleration voltage range that the analyst has to keep in mind provided that minimal x-ray counts are achieved for any meaningful mapping.
1. Theoretical x-ray resolution, in microns, by the formula $0.231 * ((E^{1.5} - E_o{}^{1.5}) / \text{density})$ where E = accelerating voltage, and E_o = critical excitation voltage:

	5 kV	10 kV	15 kV
For Si	0.88	2.9	5.53
For Al	0.80	2.55	4.81

2. Theoretical electron penetration, in microns, by formula:

$$(4120 / \text{density}) * E^{(1.265-0.0954 * \ln E)}$$

where E is accelerating voltage in MeV.

	5 kV	10 kV	15 kV
For Si	0.15	0.69	1.66
For Al	0.13	0.60	1.40

Based on these calculations the accelerating voltage has to be between 5 and 10 kV in normal circumstances where SiO_2 thickness is about 0.5 microns. Therefore, the application of this techniques is limited when defect size is down to submicron, and the value of accelerating voltage is very critical and there is always trade off between resolution and penetration which makes detection of pin hole defects under SiO_2 very difficult.

W. J. Hamilton: What size of defect will effect performance? Is the 1 micron resolution physically attainable, given the range of electrons in Si and Al?
Author: The selection of accelerating voltage is important from the resolution standpoint and from the requirement to obtain a significant P/B. It has been demonstrated experimentally that hole defect detection works best, by using a sufficiently low accelerating voltage to eliminate "background" counts from sublayer. For the devices tested in this paper, an accelerating voltage of 5 kV or lower was required to satisfy this condition. This implies a quantitative x-ray resolution limit of 0.78 micron in pure aluminum, with a corresponding electron range of 0.25 microns. Higher accelerating gave acceptable spatial resolution when image processing was used but was not as consistent when using lower accelerating voltages. Spatial resolution of a 2 micron by 1 micron hole defect was very good using an 12kV accelerating voltage, from 300X magnification to 10kX magnification (higher magnification provided better spatial resolution). At 10kX magnification, the defect was well resolved, measuring 2cm by 1cm and corresponded fairly well to SEM visual image. These results imply that submicron spatial resolution is attainable and is dependent on magnification. However, there is some question as to how far in submicron region this technique would be applicable. It is anticipated that this issue will be addressed in future studies with suitable samples. However, the only samples available for this paper had random defects that were not of suitable size to test the full limits of detectability of this technique down to the submicron region.

W. J. Hamilton: While human recognition and interpretation is enhanced by image manipulation and color display, it has been my experience (supported by the mathematics), that smoothing, averaging will improve the appearance of the data, but, in general, with a cost of spatial resolution or detection limit, or some similar parameter. For instance, a spatial average will tend to reduce the contrast of a single pixel, and thereby will tend to reduce the contrast of a single pixel, and thereby make the detection of small defects less visible. Would you comment on the "real" versus the perceived gains in the detectability of IC passivation defects?

Author: Image processing functions will tend to distort data and present danger of losing needed information. It was found that image processing functions were useful when feature sizes of interest covered large areas with a multiplicity of data i.e. high magnifications (for example, Fig. 8 versus Fig. 7). However, at lower magnification, where the defect of interest occupied only one pixel or so, the image processing functions were limited to those that would not distort needed information, such as, raising the gray scale level to the point where acceptable photographs could be obtained. Also, all the quantitative information extracted from the x-ray map were limited to unprocessed or proportionally scaled data (for suitable visual viewing).

W. J. Hamilton: Would you comment on the interpretation that the reduction in x-ray intensities around contact pads, in Fig. 4 for example, could be considered a reduction of signal due to a longer absorption path length through the elevated metallization and / or passivation layers which are seen in concomitant pad areas in the secondary electron image?
Author: The detector is off to the right at 30 degree angle to the sample surface. This effect is seen also in the linescan images of Figs. 13 and 14.

H. Oppolzer: Since the insulating passivation layers were studied at primary electron energies well above the point of unity total electron yield, what measures were taken to prevent or reduce sample charging? Was carbon coating employed, which would still allow x-ray analysis?
W. J. Hamilton: Could the data in Fig. 10 better fit the computed expectations if a 2 to 3 kV retarding potential to the primary electron beam was built up by a charging passivation layer, which shifted the "effective" kV to the left along the voltage axis?
Author: To reduce charging on the samples, all pads on the device were grounded. Further, most of the measurements were taken at sites near the bonding pads, so that the underlying aluminum metallization was connected directly to a electrical ground. Since no evidence of charging was evident with this arrangement, none of the samples were coated with carbon. Carbon coating should be evaluated to improve accuracy of the acquired data.

Further, charging does not appear to be a significant factor based on measurements correlating linescan estimates and visual analysis of SiO_2 thickness. Efforts to improve the accuracy of the results in Fig. 10 were conducted by acquiring linescan data in the vicinity of a contact area, shown in Figs. 14c and 14d. Applying absorption corrections to the intensity ratio B/A gives an improved fit to the calculated thickness curve and correlates closely with the measured SiO_2 thickness difference. In Fig. 15, the ABS B/A curve is an absorption corrected value of the intensity ratio which closely tracks the calculated 0.15 microns curve and corresponds well with the measured SiO_2 thickness difference of 0.18 microns.

W. J. Hamilton: Please comment on the accurate error estimate of ±0.05 microns mentioned in Conclusions versus poor absolute accuracy obtained?
Author: The accurate error estimate of ±0.05 microns is based on measurement of the relative thickness difference between two points on a chip, using acquired data to obtain intensity ratio between these two points and to compare / fit experimental data to calculated curves. This is best demonstrated in Fig. 15, where, as opposed to data in Fig. 10, linescan data was used to construct an experimental curve. Due to reduced spatial coverage, the x-ray count has increased statistical significance for same or reduced acquisition time as compared to the x-ray maps. Further, absorption correction factors have been applied to the intensity ratio to provide increased accuracy. This method assumes that one point, the reference point, has a known thickness and the values to be estimated are the thickness variation or difference. Based on the results in Fig. 15, the error estimate for relative thickness variation prediction was within ±0.05 microns.

With respect to absolute thickness measurements where an aluminum bonding pad is used as aluminum standard, the predicted absolute thickness of the SiO_2 film is dependent on the estimated correction factor for absorption, which is determined by iterative procedure to fit acquired data to calculated data. The accuracy for this procedure has been more difficult to determine due to lack of suitable thin film standards but has been shown to be measurable within ±0.1 microns using the penetration voltage method and the available samples which have surface roughness within ±0.1 microns.

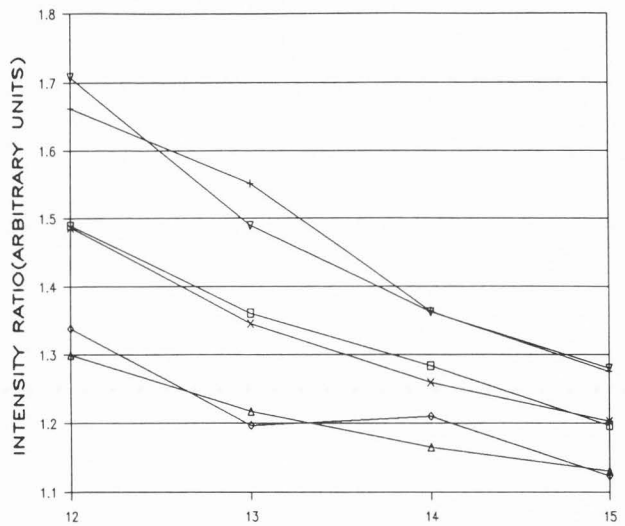

□ ABS B/A; + +d; ◇ -d; △ 0.1 μm; x 0.15 μm; ▽ 0.2 μm

Figure 15. Acquired linescan x-ray intensity ratio data corrected for absorption compared to normalized calculated intensity ratio for thickness variations of 0.1, 0.15 and 0.2 microns versus SEM accelerating voltage (+d and -d represent error bands of +0.5 and -0.5 mm on linescan plots)